

1

2 **Quantifying the individual auditory and visual brain response in**  
3 **7- month-old infants watching a brief cartoon movie**

4 Sarah Jessen<sup>1 #</sup>, Lorenz Fiedler<sup>2</sup>, Thomas F. Münte<sup>1</sup>, Jonas Obleser<sup>2</sup>

5

6 <sup>1</sup>: Department of Neurology, University of Lübeck, Lübeck, Germany

7 <sup>2</sup>: Department of Psychology, University of Lübeck, Lübeck, Germany

8

9

10

11

12 # Lead contact:

13 Dr Sarah Jessen, Department of Neurology, University of Lübeck, Ratzeburger Allee

14 160, 23562 Lübeck, Germany, Email: [sarah.jessen@neuro.uni-luebeck.de](mailto:sarah.jessen@neuro.uni-luebeck.de)

15 Phone: +49 451 3101 7449

16

17 Running title: Quantifying the individual infant brain response to real-life stimuli

18 Number of pages: 24

19 Number of figures: 8

20 Number of words (manuscript): 6240

21 Number of words (abstract): 245

22

23 **Keywords:** EEG; audiovisual; forward encoding models; temporal response function;

24 ecologically valid stimuli; developmental neuroscience

25

26 ABSTRACT

27 Electroencephalography (EEG) continues to be the most popular method to investigate  
28 cognitive brain mechanisms in young children and infants. Most infant studies rely on the  
29 well-established and easy-to-use event-related brain potential (ERP). As a severe  
30 disadvantage, ERP computation requires a large number of repetitions of items from the  
31 same stimulus-category, compromising both ERPs' reliability and their ecological validity  
32 in infant research. We here explore a way to investigate infant continuous EEG responses  
33 to an ongoing, engaging signal (i.e., "neural tracking") by using multivariate temporal  
34 response functions (mTRFs), an approach increasingly popular in adult-EEG research.  
35 N=52 infants watched a 5-min episode of an age-appropriate cartoon while the EEG signal  
36 was recorded. We estimated and validated forward encoding models of auditory-envelope  
37 and visual-motion features. We compared individual and group-based ('generic') models of  
38 the infant brain response to comparison data from N=28 adults. The generic model yielded  
39 clearly defined response functions for both, the auditory and the motion regressor.  
40 Importantly, this response profile was present also on an individual level, albeit with lower  
41 precision of the estimate but above-chance predictive accuracy for the modelled individual  
42 brain responses. In sum, we demonstrate that mTRFs are a feasible way of analyzing  
43 continuous EEG responses in infants. We observe robust response estimates both across  
44 and within participants from only five minutes of recorded EEG signal. Our results open  
45 ways for incorporating more engaging and more ecologically valid stimulus materials when  
46 probing cognitive, perceptual, and affective processes in infants and young children.

47

48 INTRODUCTION

49 Neuroimaging studies in healthy human infants are subject to severe constraints, as  
50 participants cannot follow verbal instructions, show generally short attention spans, and  
51 overall tend to be not very cooperative. As functional magnetic resonance imaging (fMRI)  
52 studies are difficult to realize in infants (Ellis & Turk-Browne, 2018),  
53 electroencephalography (EEG) continues to be the most popular method to investigate  
54 cognitive brain mechanisms in very young children and infants.

55 To analyze the EEG signal, most studies in infants rely on the use of event-related brain  
56 potentials (ERPs). Accordingly, most infant EEG paradigms have been optimized for the  
57 computation of ERPs: This method necessitates that a few, carefully selected stimulus  
58 conditions are repeated multiple times to elicit and average a stereotypical brain response  
59 (i.e., an ERP) that can then be compared between conditions or between individuals. This  
60 leads to experimental designs that are often (a) highly unnatural and (b) have difficulties  
61 capturing the infants' attention for more than a few minutes.

62 However, in recent years and with the advent of modern computational possibilities,  
63 several new approaches to analyze EEG data have become available in adult EEG research.  
64 One such approach is the so-called “neural tracking”, which seeks to compute and assess  
65 the relationship between the recorded EEG signal and an ongoing stimulus signal. The key  
66 ideas here are, first, naturally varying, non-repetitive stimuli, often movies (Bartels, Zeki,  
67 & Logothetis, 2008; Hasson, Nir, Levy, Fuhrmann, & Malach, 2004; Nishimoto et al.,  
68 2011) or naturally spoken conversation (Broderick, Anderson, Di Liberto, Crosse, & Lalor,  
69 2018; Ding & Simon, 2013; Fiedler, Wöstmann, Herbst, & Obleser, 2019), which have  
70 higher ecological validity and arguably engage the participant qualitatively differently than  
71 artificial, isolated stimuli (Hamilton & Huth, 2018; Huk, Bonnen, & He, 2018; Matusz,  
72 Dikker, Huth, & Perrodin, 2018). Second, a mathematical framework (usually a variant of  
73 the general linear model) that allows to either “reconstruct” features of such a natural  
74 stimulus based on the ongoing brain response (so-called backward or decoding models), or  
75 to “predict” the measured ongoing brain response from features of the stimulus (so-called  
76 forward or encoding models; Dayan & Abbott, 2001; Naselaris, Kay, Nishimoto, &  
77 Gallant, 2011).

78 While the use of these advanced EEG analysis approaches has become rapidly mainstream  
79 in non-human and adult human neuroscientific research, it is still rare in infant research.  
80 This is unfortunate, since they not only have yielded important new insights in adult  
81 research and are likely to offer the same potential in infant studies, but they may even

82 provide higher gains in infancy research, which suffers from notoriously low data quality  
83 and quantity. It may for instance reduce attrition rates, as experimental designs can be  
84 optimized to be highly engaging for infant participants. Rather than presenting hundreds of  
85 repetitions of very similar stimuli, which raises the additional challenge of keeping a non-  
86 cooperative participant attending to the screen, participants can be presented with  
87 constantly changing, engaging videos in which stimuli are embedded.

88 Importantly, as in adult work, infant brain research has seen an increased interest in the use  
89 of naturalistic settings over the past years. Recent research has for instance demonstrated  
90 the feasibility of investigating interpersonal neural coupling in adult-infant-interactions  
91 (Leong et al., 2017) or the use of oscillatory brain responses in analyzing responses to  
92 dynamic social information (Jones, Venema, Lowy, Earl, & Webb, 2015). While dynamic,  
93 naturalistic settings and experimental paradigms yield important new insights into how  
94 brains behave and interact in real life rather than an abstract laboratory setting, they  
95 inherently pose the additional challenge of hard-to-predict and highly variant sensory input.  
96 Being able to directly relate a constantly changing input to ongoing brain responses would  
97 therefore also be crucial for the analysis of state-of-the-art ecologically valid experimental  
98 designs.

99 One particularly promising approach to do so is the use of multivariate temporal response  
100 functions (mTRFs), which offer a mathematically simple way to link ongoing, continuous  
101 environmental signals to simultaneously recorded brain responses. In adults, mTRFs have  
102 successfully been used to track the processing of ongoing speech (e.g., Fiedler et al., 2019)  
103 as well as ongoing and naturalistic visual input (O’Sullivan, Crosse, Di Liberto, & Lalor,  
104 2017). Furthermore, Kalashnikova et al. (2018) used mTRFs in infants to analyze the  
105 processing of ongoing auditory speech signals, reporting a stronger cortical tracking for  
106 infant-directed compared to adult-directed speech (Kalashnikova, Peter, Di Liberto, Lalor,  
107 & Burnham, 2018).

108 We here demonstrate the feasibility and utility of a forward encoding modelling combined  
109 with non-repetitive complex multisensory stimulation in an infant population. We  
110 presented 7-month-old infants with a 4’48’’ long age-appropriate cartoon (one episode of  
111 the cartoon-show *Peppa Pig*) while recording the EEG. We focused our analysis on the  
112 processing of three low-level physical stimulus parameters; the auditory envelope, the  
113 motion content, and luminance. All three parameters have been amply investigated in both  
114 infants and adults and are known to elicit reliable ERP responses.

115 The auditory ERP response typically consists of a frontocentral P1–N1–P2–N2 sequence  
116 of responses, which can be clearly observed in adults and emerges in infancy and early  
117 childhood (see e.g., Wunderlich & Cone-Wesson, 2006, for a review). Compared to adults,  
118 infants tend to show a much less pronounced P1–N1 response, and the overall response is  
119 dominated by a broad P2 response (Wunderlich, Cone-Wesson, & Shepherd, 2006).

120 The infant visual ERP to complex stimuli such as objects and faces comprises three main  
121 components; the Pb, the Nc, and the Slow Wave (Webb, Long, & Nelson, 2005). In  
122 particular, the Nc response, a frontocentral negativity typically observed between 400 and  
123 800 ms after stimulus onset often linked to the allocation of attention has been amply  
124 investigated (de Haan, Johnson, & Halit, 2003; Reynolds & Guy, 2012).

125 If we were successful in estimating auditory and visual brain responses using a forward  
126 encoding model approach, we expect response functions comparable to classical evoked  
127 brain responses. Furthermore, since the combined use of auditory and visual regressors  
128 provides more information compared to the use of either regressor alone, we expected a  
129 more consistent and reliable response function when using auditory and visual regressors  
130 in one model.

131 Finally, while it is common in adult studies using mTRFs to compute individual response  
132 functions based on a subset of the available data, due to the limited amount of data available  
133 in the infant cohort we aimed to explore the potential benefit from relying on a “generic”  
134 response function (Di Liberto & Lalor, 2017), that is, an average response function  
135 computed across participants. Hence, we computed an averaged response function over  $n-1$   
136 participants and used this response function to model responses in the  $n$ th participant (i.e.  
137 leave-one-out cross validation). We directly contrasted results obtained with these two  
138 approaches on the present data set.

139

## 140 METHODS

141 *Infant participants.* Fifty-two 7-month-old infants were included in the final sample (age:  
142  $213 \pm 8$  days [mean  $\pm$  standard deviation (SD)]; range: 200-225, 24 female). Not untypical  
143 for infant studies (Stets, Stahl, & Reid, 2012), an additional 39 infants had been tested but  
144 could not be included in the final sample. Note also that directly prior to the experiment  
145 reported here, infants had already participated in a 5–10-minute-long ERP experiment on  
146 visual emotion perception (see below), further contributing to the drop-out rate since  
147 infants often became fussy or tired after the first experiment. In detail, infants were

148 excluded because they did not watch the complete video (n=24); were too fussy to watch  
149 the video at all (n=10); did not contribute at least 100 s of artifact-free data (n=3); had  
150 potential neurological problems (n=1); or because of technical problems during the  
151 recording (n=1).

152 All infants were recruited via the maternity ward at the local hospital (Universitätsklinikum  
153 Schleswig-Holstein); were born full-term (38–42 weeks gestational age); had a birth weight  
154 of at least 2500 g; and had no known neurological deficits. The study was conducted  
155 according to the declaration of Helsinki, approved by the ethics committee at the University  
156 of Luebeck, and parents provided written informed consent.

157 *Adult reference sample.* In addition, we collected data from a reference sample of n = 33  
158 adult participants. Data from n=5 were excluded due to technical difficulties during the  
159 recording (n=2) or failure to contribute at least 100 s of artifact-free data (n=3), leading to  
160 a final sample of n=28 (mean age: 50 years; range: 21–69, 16 female).

161 *Stimulus.* As stimulus material we used one episode (duration 4'48'', that is, 269 s or 6451  
162 frames) of the cartoon show Peppa Pig (“Peppa Pig–The new car”), an age-appropriate  
163 cartoon featuring a family of pigs and their daily life. Sound and visual parameters were  
164 not manipulated in any way.

165 *Procedure–Infants.* After arrival in the laboratory, parents and infant were familiarized  
166 with the environment and parents were informed about the study and signed a consent form.  
167 The EEG recording was prepared while the infant was sitting on his/her parent’s lap. For  
168 recording, we used an elastic cap (BrainCap, Easycap GmbH) in which 27 Ag/AgCl-  
169 electrodes were mounted according to the international 10-20-system. An additional  
170 electrode was attached below the infant’s right eye to record the electrooculogram. The  
171 EEG signal was recorded with a sampling rate of 250 Hz using a BrainAmp amplifier and  
172 the BrainVision Recorder software (both Brain Products).

173 For the EEG recording, the infant was sitting in an age appropriate car seat (Maxi Cosi  
174 Pebble) positioned on the floor. As part of a larger study, a t-shirt was positioned over the  
175 chest area of the infants. The t-shirt had either previously been worn by the infant’s mother  
176 (n=19) or by the mother of a different same-aged infant (n=14) or had not been worn before  
177 (n=19). This modulation was not of main interest to the present study and will not be  
178 analyzed or reported here in further detail.

179 In front of the infant (approximately 60 cm from the infant’s feet), a 24-inch monitor with  
180 a refresh rate of 60 Hz was positioned at a height of about 40 cm (bottom edge of the

181 screen). Left and right of the monitor, loudspeakers (Logitech X-140) were positioned and  
182 set to a comfortable level of loudness. When the infant was attending to the screen, the  
183 video was started and played without interruption until the end of the episode. The parent  
184 was seated approximately 1.5 m behind the infant and was instructed not to interact with  
185 the infant during the video. In case the infant became too fussy and started crying during  
186 the video, the video was aborted and the infant was excluded from further analysis.

187 Before this video presentation, infants had been presented with a series of photographs  
188 displaying happy and fearful facial expressions as part of the larger, maternal-odor study.  
189 Again, the results of this part of the study will not be further analyzed here.

190 *Procedure—Adults.* Adult participants were presented with the same “Peppa Pig” movie  
191 after they had already participated in one of several unrelated EEG studies. They were  
192 informed about the study and signed a consent form. For recording the EEG signal, we  
193 used 64 Ag/AgCl active scalp electrodes positioned in an elastic cap according to the  
194 international 10-20-system. The EEG signal was recorded with a sampling rate of 1000 Hz  
195 using an ActiChamp amplifier and the BrainVision Recorder software (Brain Products).

196 Adult participants sat in a soundproof and electrically shielded chamber (Desone) in a  
197 comfortable chair approximately 1 m away from a 24-inch monitor with a refresh rate of  
198 60 Hz on which the video was presented. Sound was presented from the same loudspeaker  
199 models used in the infant study, also positioned left and right to the screen (Logitech X-  
200 140).

201 *Analysis.* Unless noted otherwise, the analysis protocol was identical for infant and adult  
202 data. We analyzed the data using Matlab 2013b (The MathWorks, Inc., Natick, MA), the  
203 Matlab toolbox FieldTrip (Oostenveld, Fries, Maris, & Schoffelen, 2011), and the  
204 multivariate temporal response function (MTRF) toolbox (Crosse, Di Liberto, Bednar, &  
205 Lalor, 2016).

206 *Preprocessing.* The data were referenced to the average of all electrodes (mean reference),  
207 filtered using a 100-Hz-lowpass and a 1-Hz-highpass filter, and segmented into 1-sec-  
208 epochs. To detect epochs contaminated by artifacts, the standard deviation was computed  
209 in a sliding window of 200 msec. If the standard deviation exceeds 80 mV at any electrode,  
210 the entire epoch was discarded, and if less than 100 artifact-free epochs remained, the  
211 participant was excluded from further analysis. An independent component analysis (ICA)  
212 was computed on the remaining epochs. Components were inspected visually by a trained  
213 coder (S.J.) and rejected if classified as artefactual (infants:  $5 \pm 2$  components per  
214 participant [mean  $\pm$  SD], range 1–10; adults:  $26 \pm 5$ , range 11–36). A 1–10 Hz bandpass

215 filter was applied to the cleaned data. Adult data were downsampled to the infant-data  
216 sampling frequency of 250 Hz.

217

218 *Extraction of stimulus regressors.* Regressors characterizing motion, luminance,  
219 and the sound envelope were extracted from the stimulus video. Exemplary excerpts of  
220 audio, luminance, and motion regressors are shown in Fig 1B.

221 To compute a regressor of average luminance across all pixels, the weighted sum  
222 of the rgb values for each frame was computed using Matlab (Bartels et al., 2008).

223 To compute a regressor of average motion across all pixels, each video frame was  
224 converted to grey-scale, and the difference between two consecutive frames was computed.  
225 Then, the mean across all pixels for which this difference was larger than 10 (to account  
226 for random noise, see e.g. Jessen & Kotz, 2011; Pichon, de Gelder, & Grèzes, 2009) was  
227 computed.

228 To compute a regressor of sound envelope, the audio soundtrack of the video was  
229 extracted and submitted to the NSL toolbox, an established preprocessing pipeline  
230 emulating important stages of auditory peripheral and subcortical processing (Ru, 2001).  
231 The output of this toolbox resulted in a representation containing band-specific envelopes  
232 of 128 frequency bands of uniform width on the logarithmic scale with center frequencies  
233 logarithmically spaced between 0.1 and 4 kHz. To obtain the broadband temporal envelope  
234 of the audio soundtrack, these band-specific envelopes were then summed up across all  
235 frequencies to obtain one temporal envelope. Following earlier own and others'  
236 approaches, we used the first derivative of the half-wave rectified envelope as the final  
237 audio regressor (for details see Fiedler et al., 2017). The result is a pulse-train-like series  
238 of peaks where, across frequency bands, the acoustic energy rises most steeply, reflecting  
239 “acoustic edges” such as syllable onsets.

240

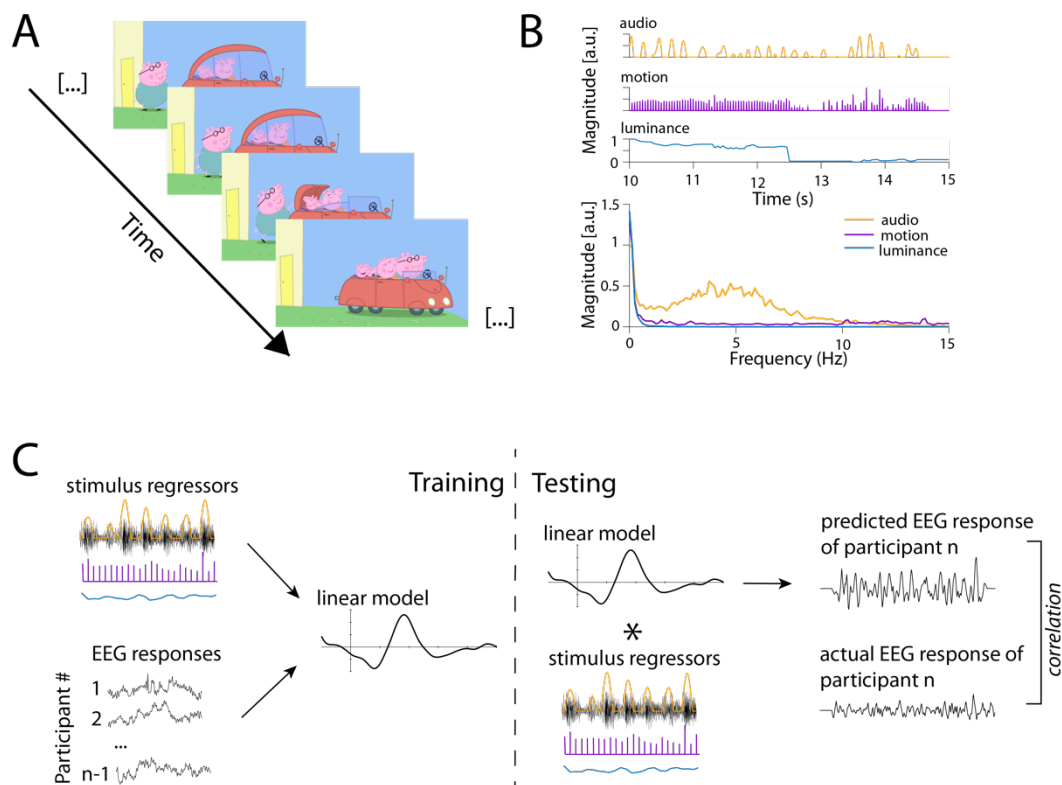
241 *Stimulus parameters.* As expected for a child-friendly cartoon movie, frame-to-frame  
242 fluctuations in luminance were small. On average, the change in luminance from one frame  
243 to the next was 0.35 units per frame (range 0–53, median = 0.05). Note that this deviates  
244 from previous studies where the entire dynamic range of luminance (i.e., black to white)  
245 was used to quantify the temporal response function in the adult EEG response (e.g., Lalor,  
246 Pearlmuter, Reilly, McDarby, & Foxe, 2006; Vanrullen & MacDonald, 2012) or in non-  
247 human animal electrophysiological responses (Ringach & Shapley, 2004). In contrast, the  
248 luminance-derived motion regressor yielded sizable variance, with a mean frame-to-frame  
249 change of 38 units (range 0–192, median = 36).



250 In sum, while variance in the luminance regressor was small, both motion and  
 251 audio regressors showed considerable and promising degrees of variance.

252 Lastly, all regressors were downsampled (audio) and interpolated (motion,  
 253 luminance), respectively, to the EEG sampling frequency of 250 Hz. In all regressors, time  
 254 periods in which no EEG data was available as a result of artefact rejection during  
 255 preprocessing were zero-replaced. Finally, EEG data and physical regressors were aligned  
 256 and available for the linear model analysis.

257



258

259 *Figure 1. Physical properties of stimulus regressors.* A) shows four exemplary stills from  
 260 the movie used as stimulus material. B) shows an example of a 5-s-long stretch of the audio  
 261 (orange), motion (purple), and luminance regressors (blue). Below, the frequency spectrum  
 262 of the stimulus regressors is depicted; while frequencies < 10 Hz appear to be dominant in  
 263 the audio regressors, no such dominance can be observed for the other regressors. C) shows  
 264 an overview of the analysis approach. During training, stimulus regressors and the EEG  
 265 signal of n-1 participants was used to compute a generic response function (left part).  
 266 During testing, this generic response function was used to predict the EEG response of the  
 267 nth participant, which was then compared to the actual EEG response of that participant.  
 268 See main text for further details.

269

270 *Temporal response functions (TRF).* To quantify the degree to which the measures EEG of  
 271 7-month-olds (as well as adults) can be expressed as a linear response to stimulus features,

272 we used regularized regression (with ridge parameter  $\lambda$ ) as implemented in the mTRF  
273 toolbox (Crosse et al., 2016). The key idea here is to estimate a temporal response function  
274 (TRF), that is, a set of time-lagged weights  $g$ , with which a regressor  $s$  (here, the physical  
275 stimulus features) would need to be convolved (i.e. multiplied and summed) in order to  
276 optimally predict the measured EEG response  $r$ .

277 More specifically, we used a forward encoding model approach. In a first pass, we  
278 aimed to maximize the predictive accuracy of such a model by estimating so-called  
279 “generic” models, that is, we predicted the EEG data of an  $n$ th participant based on a  
280 “generic” temporal response function (TRF) from  $n-1$  participants to the auditory or visual  
281 stimulus signal. Since changes in the EEG signal are not likely to occur simultaneously  
282 with changes in the stimulus signal but rather with an (unknown) time lag, predictions were  
283 computed over a range of time lags between 200 ms earlier than the stimulus signal and  
284 1000 ms later than the stimulus signal.

285 *Choosing the optimal regularization parameter  $\lambda$ .* To obtain the optimal regularization  
286 parameter  $\lambda$  for each stimulus regressor separately, as well motion and audio  
287 simultaneously, we trained the respective model on a variety of  $\lambda$  values between  $10^{-5}$  and  
288  $10^5$ , increasing the exponent in steps of 0.5, and used the resulting models to predict the  
289 EEG signal for each participant. We then computed the mean response function across  $n-1$   
290 participants and used this response function to predict EEG response of the  $n$ th participant  
291 (i.e.,  $n$ -fold leave-one-out crossvalidation). Finally, we computed the predictive accuracy  
292 (i.e., Pearson’s correlation coefficient  $r$  between the predicted EEG response and the actual  
293 EEG response) for each participant, resulting in one accuracy value for each electrode (27  
294 for infants, 64 for adults) per participant and stimulus parameter for each  $\lambda$  value. For each  
295 participant, stimulus parameter, and electrode, we selected the  $\lambda$  value maximizing  
296 *predictive accuracy*. Based on these values, we obtained the mean regularization parameter  
297  $\lambda$  value across all electrodes and participants (see Table S1).

298 These optimal  $\lambda$  parameters were used in the following to train the model, resulting  
299 in separate response functions for each stimulus parameter. For each of the three physical  
300 stimulus parameters (luminance, motion, audio) we computed a separate model. In  
301 addition, we computed a model using both, motion and audio, as regressors (“joint audio-  
302 motion model”). We chose not to include luminance in this model, as the regressor for  
303 luminance did not yield any reliable model in itself (see results).

304 *Evaluation of temporal response functions.* For statistical evaluation of the resulting  
305 response functions, we computed a cluster-based permutation test with 1000

306 randomizations, testing the obtained response functions against zero. A cluster was defined  
307 along the dimensions time and electrode position, with the constraint that a cluster had to  
308 extend over at least two adjacent electrodes. A type-1-error probability of less than .05 was  
309 ensured for all clusters.

310 In addition, to assess internal validity of our model predictions on an individual  
311 basis, we computed three different predictive accuracies per participant. First, for each  
312 participant  $n$ , we computed the correlation between the predicted response generated on a  
313 model trained on  $n-1$  participants and the actual EEG response of  $n$  (“generic model”).

314 Second, rather than relying on the generic model based on  $n-1$  participants, we  
315 computed an individual response function for each participant (“individual model”). To  
316 that end, 80 % of the available data for a given participant were used to train the model,  
317 and the resulting response function was then correlated with the response observed in the  
318 remaining 20 % of the data.

319 Third, a *permuted* or null predictive accuracy (“shifted control”) was obtained.  
320 Before calculating accuracy this way, we shifted the actual EEG response for participant  $n$   
321 in steps of 2 s (in order to ensure to exceed the potential autoregressive structure of the  
322 EEG data) and computed the correlation between the shifted EEG signal and the predicted  
323 response, based on the generic model trained on  $n-1$  participants.

324

## 325 RESULTS

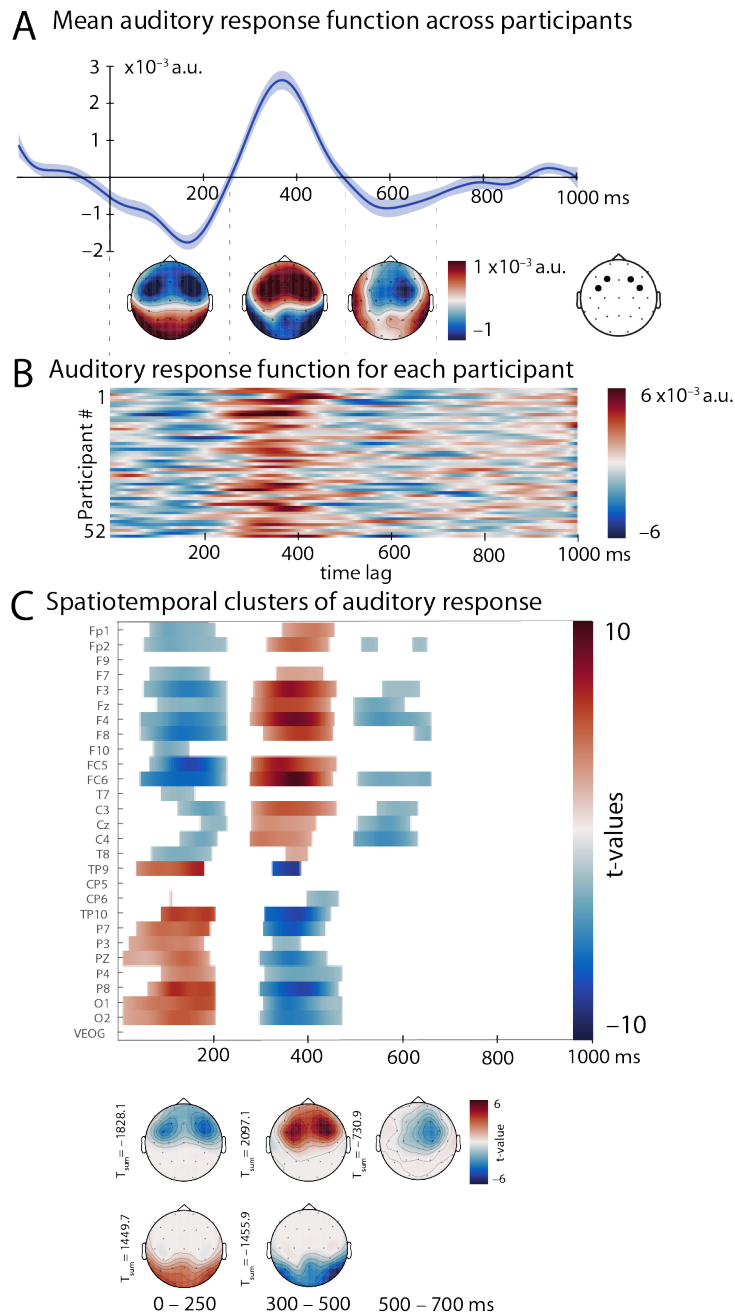
326 *Temporal response function.* We computed a generic temporal response function for each  
327 stimulus regressor as well as the audio and motion regressor combined (joint audio-motion  
328 model).

329 We observed a clearly defined response function using the audio regressor (Figure  
330 2 for infants and Figure S2 for adults) and the motion regressor (Figure 3 and Figure S3 for  
331 adults), while no clear response function could be obtained using the luminance regressor  
332 for either infants or adults (Figure S1). While Figures 2 and 3 show the respective response  
333 functions obtained from a model which included both regressors (joint audio-motion  
334 model), comparable response functions resulted when using either of the regressors in  
335 isolation.

336 Interestingly, the observed response function did not only become visible in the  
337 average response function, but also for the vast majority of participants on an individual  
338 level (Figure 2B and 3B). Furthermore, note that while a clearly defined response was

339 visible for both, the audio and motion regressor, the amplitude of the response function for  
340 the motion regressor was much smaller compared to the amplitude of the audio response  
341 function.

342



343

344 *Figure 2. Auditory response function (using motion and audio regressor simultaneously)*  
345 *for infant participants.* A) shows the mean mTRF (mean  $\pm$  within-subject SEM) computed  
346 across all participants, averaged over FC5, FC6, F3, and F4, and topographic  
347 representations for 0–250 ms, 250–500 ms, and 500–700 ms with electrodes included in  
348 the above-shown average marked by black dots. B) shows the auditory response  
349 function for each individual infant. C) displays the results of the cluster-based permutation test,

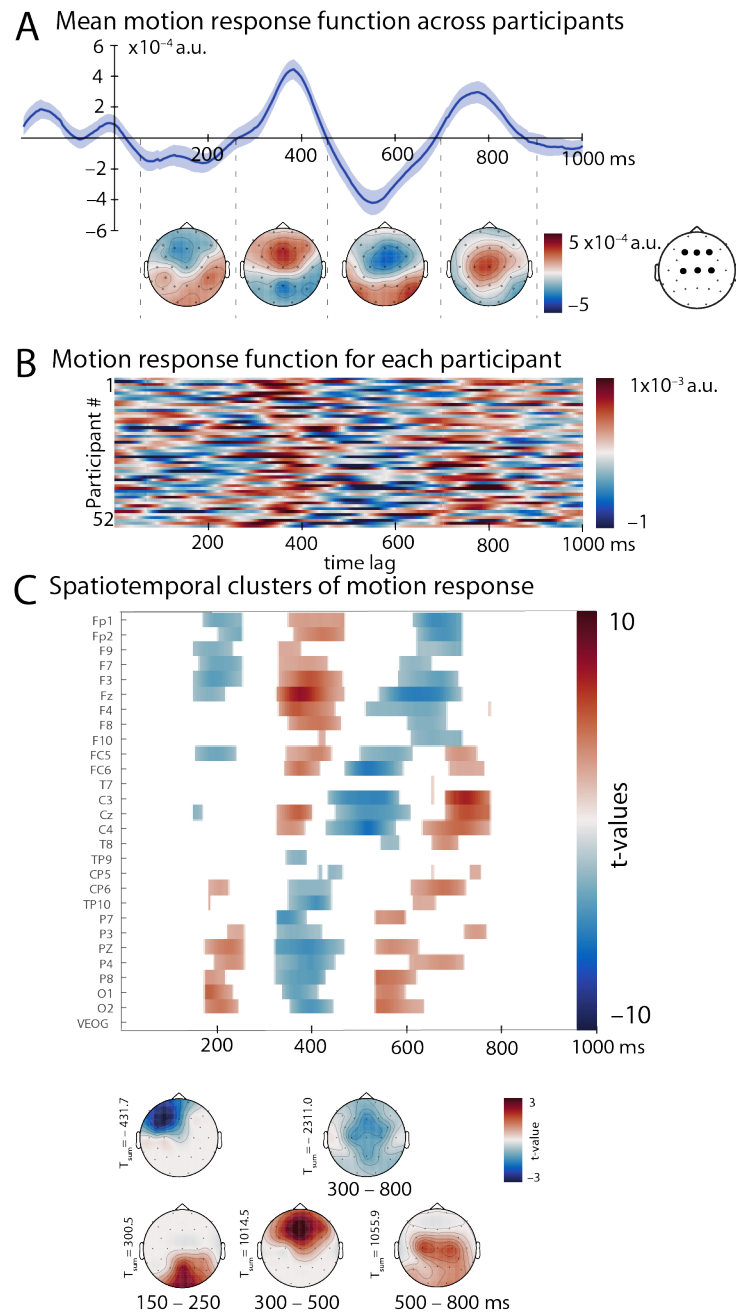
350 comparing the response function shown in A) and B) to zero. Positive deviations are  
351 displayed in red, while negative deviations are shown in blue. In the bottom part of C), the  
352 same clusters as in the top part of C) are shown as topographic distributions, along with the  
353 summed t-value across the cluster.

354 *Comparing infant and adult brain responses.* When directly comparing infant and adult  
355 response functions (Figure 4), similarities as well as striking differences emerge. Overall,  
356 amplitudes of the response functions are comparable for infants and adults, both showing  
357 the already mentioned larger amplitudes for audio regressors and smaller amplitudes for  
358 motion regressors. For both, infants and adults, the auditory response function is marked  
359 by a prominent frontocentral positivity (250–500 ms for infants, 300–450 ms for adults).  
360 While this response appears to be slightly longer for infants, overall, both latency and  
361 topography indicate a comparable response for infants and adults. In contrast, the infant  
362 auditory response function lacks a second, earlier and more central positivity, which can  
363 be observed between 150 and 250 ms in the adult auditory response function.

364 For the motion response function, both infants and adults show two frontal /  
365 frontocentral positivities (250–450 and 700–900 ms for infants and 250–350 and 450–550  
366 ms for adults). Hence, infants and adults show a comparable response, though the infant  
367 response appears to be much slower and less temporally modulated.

368 *Cluster-based permutation test.* We computed a cluster-based permutation test comparing  
369 the temporal response function obtained using the motion, luminance, and audio regressor  
370 as well as the motion and audio regressor simultaneously. We did not observe any  
371 significant cluster using the luminance regressor for either infants or adults. In contrast, we  
372 did obtain multiple significant clusters, indicating a positive or negative deviation from  
373 zero, for the motion and audio regressor, both when included separately as well as in  
374 combination (see supplementary material for a full list of the results of the cluster-based  
375 permutation test using audio and motion regressor separately as well as in combination for  
376 infants and adults, Figure 2C and 3C for infant results and S2C and S3C for adult results).  
377 The resulting clusters confirm the deflections observed in the auditory and motion response  
378 function (Figure 2A and 3A, respectively).

379



380

381 *Figure 3. Motion response function (using motion and audio regressor simultaneously) for*  
 382 *infant participants.* A) shows the mean mTRF (mean  $\pm$  SEM) computed across all  
 383 participants, averaged over F3, Fz, F4, C3, Cz, and C4, and topographic representations for  
 384 50–250 ms, 250–450 ms, 450–700 ms, and 700–900 ms with electrodes included in the  
 385 above-shown average marked by black dots. B) shows the motion response function for  
 386 each individual infant. C) displays the results of the cluster-based permutation test,  
 387 comparing the response function shown in A) and B) to zero. Positive deviations are  
 388 displayed in red, while negative deviations are shown in blue. In the bottom part of C),  
 389 the same clusters as in the top part of C) are shown as topographic distributions, along with  
 390 the summed t-value across the cluster.

391

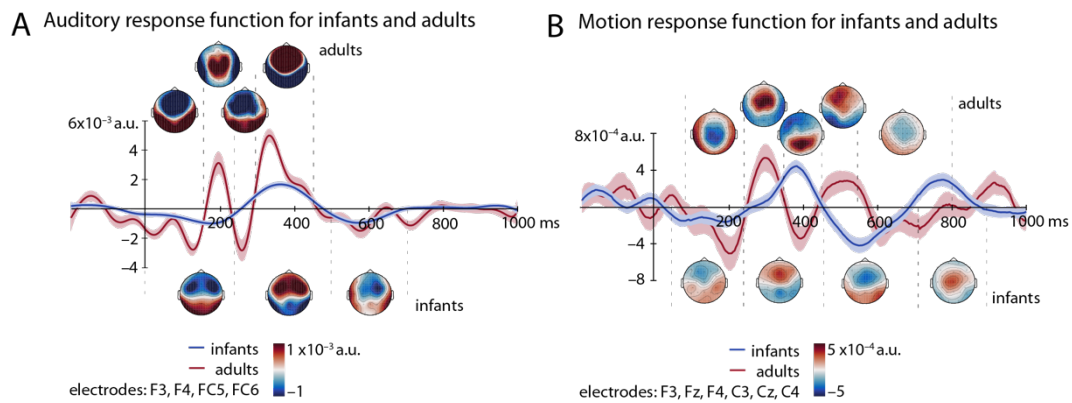


*Figure 4. Comparison of infant and adult response functions.* Mean mTRF for infant (in blue) and adult (in red) participants are shown for the audio regressor (A) and the motion regressor (B). The infant response functions and topographical representations are identical to those shown in Fig 2A and 3A for audio and motion regressors, respectively. Responses are averaged across the same electrodes for adults and infants, namely FC5, FC6, F3, and F4 for A) and F3, Fz, F4, C3, Cz, and C4 for B). The topographic representations of adult responses correspond to those in the supplementary material, namely 50–150 ms, 150–250 ms, 250–300 ms, and 300–450 ms for A) and 50–250 ms, 250–350 ms, 350–450 ms, 450–550 ms, and 550–800 ms for B).

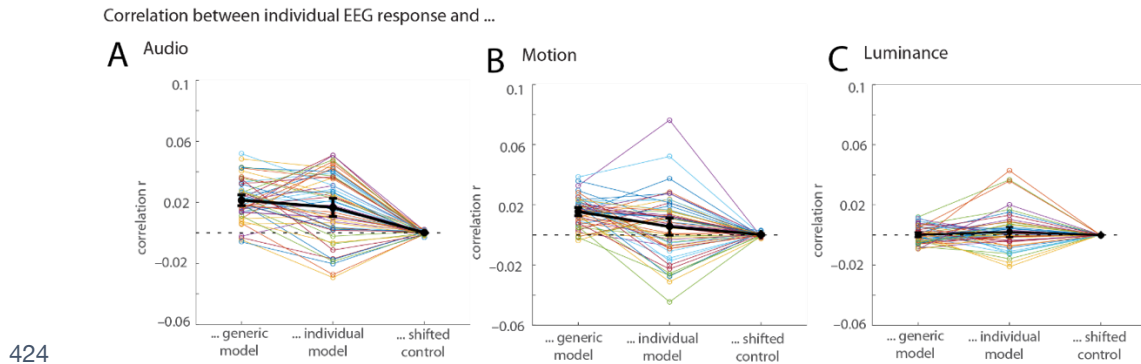
*Generic vs. individual response functions.* The results discussed above rely on a generic model computed based on data from  $n-1$  participants in order to predict the  $n$ th participant (see Di Liberto & Lalor, 2017). An alternative approach (and in fact preferable, if enough data for per subject is available; e.g., Fiedler et al., 2019; O’Sullivan et al., 2017) computes an individual model based on a subset of an individual’s data and compare the resulting predictions to the remaining data.

As expected, individual models showed a larger variance compared to the generic model (Figure 5–7; see S4 and S5 for data from adult participants), but both, generic model and individual model result in correlations clearly above zero (with the exception of luminance, where no reliable prediction was possible for either mode, see Figure 5C).

When both, audio and motion regressor were included (Figure 6), the generic model resulted in a higher correlation compared to the individual model for infant participants ( $t(51)=3.76, p<.001$ ); 37 participants showed a higher correlation with the generic model while only 15 participants showed a higher correlation with the individual model. When using only the motion regressor (Figure 5B), the correlations were also higher for the generic compared to the individual model ( $t(51)=3.50, p<.001$ ), while for the auditory regressor (Figure 5A), this difference was less pronounced ( $t(51)=1.82, p=.07$ ).

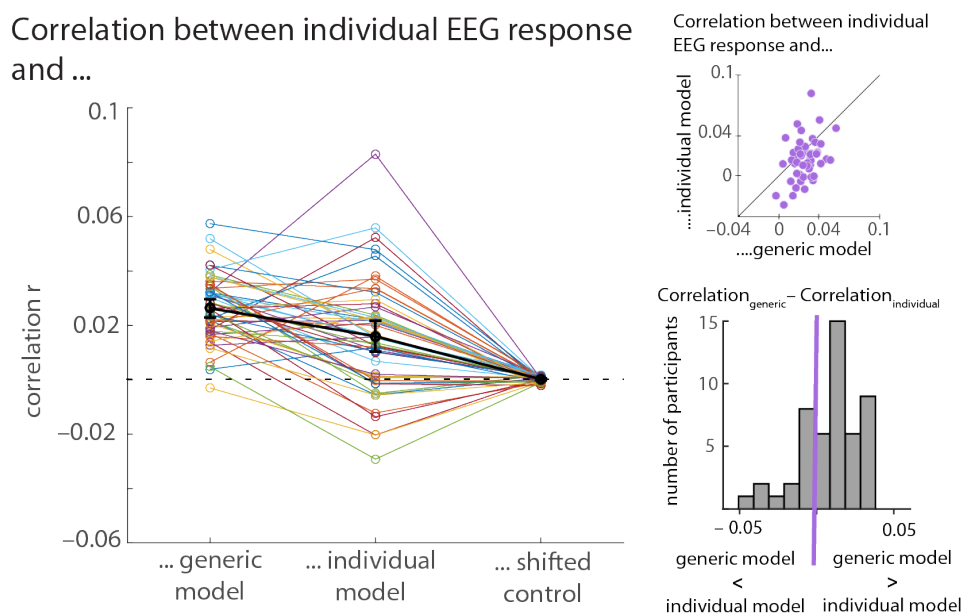
420 As a control analysis, a generic model using temporally shifted (i.e., purposefully  
421 misaligned) versions of the actual EEG signal (1,000 iterations) did yield substantially  
422 lower predictive accuracy values.

423



425 *Figure 5. Predictive Accuracy (r) between model and EEG response for infant participants.*  
426 The recorded individual EEG response was correlated with three different parameters using  
427 Pearson's correlation coefficient for the audio regressor (A), motion regressor (B), and  
428 luminance regressor (C). On the left, the correlation between the recorded EEG responses  
429 of participant n and the response predicted by the generic model based on the remaining n-  
430 1 participants is shown for each participant. In the middle, the correlation between the  
431 model trained on the first 80 % of the data available for each participant and used to predict  
432 the remaining 20 % from that participant and the actual EEG response recorded from that  
433 participant is shown. The right column shows the correlation between the prediction  
434 generated by the generic model and the recorded EEG data shifted in a circular way in steps  
435 of 2 s as a control condition (averaged over all possible shifts). Correlations are shown for  
436 each infant participant (in colors) as well as the mean correlation with 95% CI (confidence  
437 interval) across all participants (in black).

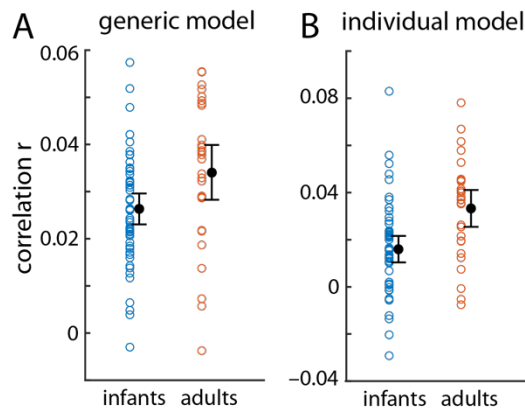
438





440 *Figure 6. Predictive accuracy for modelled and observed EEG response for infant*  
441 *participants in a joint audio–motion model.* The left part of the figure shows the correlation  
442 (based on Pearson’s correlation coefficient) between the recorded EEG signal and the EEG  
443 responses predicted based on the generic model (left column), the individual model (middle  
444 column), and a shifted control condition (right column, see text). The two plots on the right  
445 hand visualize a comparison between the generic and the individual model. In the top plot,  
446 each purple dot indicates the difference between the correlation with the generic model and  
447 the correlation with the individual model. Hence, a purple dot in the right bottom part of  
448 the graph indicates an individual with a higher correlation for the generic compared to the  
449 individual model, while a purple dot in the top left part indicates an individual with a higher  
450 correlation for the individual compared to the generic model. The bottom plot displays the  
451 same information in a bar graph; individuals having a higher correlation for the generic  
452 model have a positive difference and hence fall to the right of the zero-threshold marked in  
453 purple while those with a higher correlation for the individual model have a negative  
454 difference and fall to the left of the zero-threshold.

455



456

457 *Figure 8. Predictive accuracy for infants and adults in a joint audio–motion model.* A)  
458 shows the individual correlations using Pearson’s correlation coefficient for infants (blue)  
459 and adults (orange) using the generic model. B) shows the individual correlations using  
460 Pearson’s correlation coefficient for infants (blue) and adults (orange) using the individual  
461 model. Mean accuracies with 95 % confidence intervals are shown in black.

462

## 463 DISCUSSION

464 We investigated the use of a variant of forward encoding models (multivariate temporal  
465 response functions, mTRFs) to analyze infant brain responses to a continuous complex  
466 audiovisual stimulus, namely a 5-minute cartoon movie. We observed clearly defined  
467 response patterns to both the auditory as well as the motion content, but no predictive  
468 response function for changes in luminance was found.

469 Our results demonstrate that the simultaneous acquisition of individual brain  
470 responses to different sensory modalities is possible in the infant brain, opening new  
471 avenues for ecologically valid multisensory research paradigms in developmental  
472 neuroscience. Furthermore, our results suggest that a generic model derived from a larger

473 set of unrelated infant data is as good or slightly better compared to an individual model in  
474 predicting the individual brain response, especially in cases where only limited data is  
475 available. This points to the further utility of such an approach in developmental and at-  
476 risk populations.

477 *Motion and Audio.* For both, motion and audio information in the cartoon movie, we found  
478 a clearly defined response in both infants and adults. The observed responses are largely  
479 consistent with patterns typically reported in more traditional event-related brain potentials.  
480 The frontocentral negativity between 450 and 700 ms for instance observed in the infant  
481 brain responses linked to the motion regressor corresponds in timing, shape, and  
482 topography to the Nc component, an infant ERP component that can routinely be observed  
483 in visual paradigms and has been linked to attention allocation (Webb et al., 2005).  
484 Likewise, the bifocal frontal positivity observed in the infants' brain response linked to the  
485 auditory envelope shows a strong similarity to the commonly reported P2 response in infant  
486 auditory brain responses (Wunderlich et al., 2006).

487         The direct comparison of infant and adult brain responses (Figure 4) may provide  
488 insight into the developmental changes. In response to the auditory envelope, both infants  
489 and adults show a prominent frontal negativity peaking around 400 ms. Notably, however,  
490 the adults show an additional central positivity around 200 ms, which is missing in the  
491 infant response. This corroborates and replicates known developmental changes commonly  
492 observed in auditory evoked responses when comparing infants and adults (Wunderlich &  
493 Cone-Wesson, 2006). Considering the motion response, the correspondence between infant  
494 and adult response is less straight-forward. While the adult response is characterized by  
495 two frontocentral positivities, one peaking around 300 ms and the other around 500 ms, the  
496 infant response is dominated by one frontocentral peak around 400 ms.

497         Importantly, we used both, generic response functions as well as individual  
498 response functions to predict the EEG signal. When using both, the motion and the auditory  
499 regressor, performance was significantly better for the generic compared to the individual  
500 model. When using only the auditory regressor, the same pattern was visible but the  
501 difference only marginally significant. Note, however, that both, generic and individual  
502 models generated predictions that were significantly above chance level. This demonstrates  
503 two important things. First, five minutes of EEG recording are sufficient to compute  
504 reliable models, both on an individual level as well as across participants as a generic  
505 model. This is not only true for EEG data obtained from healthy adults but also for data  
506 obtained from populations providing notoriously noisy signal, such as infants. Second,  
507 brain responses across participants, both infants and adults, are sufficiently similar to

508 generate a model that can successfully predict a new infant's brain response, yielding even  
509 better outcomes compared to the individual model.

510 *Limitations and future studies.* The present study provides an important step and proof of  
511 feasibility for using mTRFs to analyze infant EEG data in response to complex and  
512 dynamic audiovisual stimulus material. This offers a whole host of new possibilities in the  
513 investigation of infant's brain responses in their natural environment.

514 One important feature of the present study is that we used the unmanipulated  
515 cartoon video material. While this makes for an ecologically valid and easy-to-obtain  
516 stimulus, it comes with the caveat of a lack of control for stimulus properties.  
517 Notably, while we did observe a clear-cut response to the motion and the auditory  
518 regressor, we did not find a reliable response to the changes in luminance. The most likely  
519 explanation for this discrepancy is the lack in variance in the luminance content. While the  
520 motion and the auditory regressor showed large-amplitude changes throughout the video  
521 (e.g., average motion change between frames = 38 units), average luminance of this cartoon  
522 movie remained fairly constant (average luminance change between frames = 0.35 units).  
523 Previous studies targeting neural responses to luminance change (in adults) typically used  
524 considerably more pronounced black–white contrast (Lalor et al., 2006; Vanrullen &  
525 MacDonald, 2012). Hence, the luminance changes in the stimulus material were likely too  
526 small to elicit any robust change in brain response. Future studies explicitly varying the  
527 luminance content are therefore necessary to investigate the applicability of mTRFs to  
528 other visual stimulus parameters in infants.

529 Also, we operationalized motion as change in pixel from one frame to the next.  
530 This means that the motion regressor not only reflected the actual motion of the objects and  
531 persons depicted in the video but also cuts in the video. For the present purpose, we did not  
532 differentiate between these two possibilities of motion.

533 Building upon the present results, a next step would therefore be to purposefully  
534 manipulate such parameters. By using stimulus material designed to encompass a larger  
535 variance in luminance and/or no cuts in the video, it should for instance be possible to  
536 observe brain response to changes in luminance and motion responses that can be clearly  
537 linked to actual motion rather than video cuts. Such an approach could for instance provide  
538 valuable new insights into the processing of biological motion (Marshall & Shipley, 2009;  
539 Reid, Hoehl, & Striano, 2006).

540 Furthermore, in the present study, we did not contrast different conditions, neither  
541 within infant nor between different groups of infants. Having demonstrated the feasibility

542 of using encoding models to model brain responses for this type of complex audiovisual  
543 stimuli, the next step would certainly be to utilize this approach to investigate differences  
544 in processing between (a) different types of stimulation or (b) different groups of infants.

545 A first step in using mTRFs to contrast different continuous stimulus signals has  
546 been done by Kalashnikova et al. (2018), who compared the processing of infants vs. adult  
547 directed speech in 7-month-olds. Future studies could encompass more complex  
548 naturalistic scenarios, using for instance audiovisual video material. More importantly,  
549 mTRFs can also be used to investigate brain responses in live interactions, in which the  
550 live input the infant receives is recorded and used as a regressor in the subsequent analysis.  
551 Such an approach would provide an important tool in investigating the neural bases of  
552 social interactions.

553 *Conclusion.* The present data demonstrate that forward encoding models based on the  
554 multivariate temporal response function (mTRF) pose a valuable and versatile tool in  
555 quantifying and disentangling complex audiovisual brain responses and the according  
556 perceptual processes in infancy. Our results open way for applications to a variety of  
557 research areas not only in early development, but also in other special populations  
558 characterized by short attention spans and low cooperativeness, including research in  
559 severely impaired neurological patients. New paradigms could not only entail complex  
560 multisensory perception, but extend to dynamic social interactions. As such, mTRF  
561 approaches to infant data analysis will allow developmental researchers to devise more  
562 engaging and thereby more easily applicable experimental set-ups for infancy research.

563

#### 564 ACKNOWLEDGEMENTS

565 We thank all the families for participating, Leonie Emmerich, Aylin Ulubas, Franziska  
566 Scharata, and Anne Hermann for help with the data acquisition, and the German Research  
567 Foundation (DFG) for funding to SJ (JE 781/1-1 & 2).

#### 568 DATA ACCESSIBILITY.

569 Data will be made available upon publication.

570

571 BIBLIOGRAPHY

- 572 Bartels, A., Zeki, S., & Logothetis, N. K. (2008). Natural vision reveals regional  
573 specialization to local motion and to contrast-invariant, global flow in the human  
574 brain. *Cerebral Cortex*. <https://doi.org/10.1093/cercor/bhm107>
- 575 Broderick, M. P., Anderson, A. J., Di Liberto, G. M., Crosse, M. J., & Lalor, E. C.  
576 (2018). Electrophysiological Correlates of Semantic Dissimilarity Reflect the  
577 Comprehension of Natural, Narrative Speech. *Current Biology*.  
578 <https://doi.org/10.1016/j.cub.2018.01.080>
- 579 Crosse, M. J., Di Liberto, G. M., Bednar, A., & Lalor, E. C. (2016). The Multivariate  
580 Temporal Response Function (mTRF) Toolbox: A MATLAB Toolbox for Relating  
581 Neural Signals to Continuous Stimuli. *Frontiers in Human Neuroscience*.  
582 <https://doi.org/10.3389/fnhum.2016.00604>
- 583 Dayan, P., & Abbott, L. (2001). *Theoretical Neuroscience: Computational and*  
584 *Mathematical Modeling of Neural Systems*. Cambridge, MA: MIT Press.
- 585 de Haan, M., Johnson, M. H., & Halit, H. (2003). Development of face-sensitive event-  
586 related potentials during infancy: a review. *International Journal of*  
587 *Psychophysiology*, 51(1), 45–58. Retrieved from  
588 <http://www.ncbi.nlm.nih.gov/pubmed/14629922>
- 589 Di Liberto, G. M., & Lalor, E. C. (2017). Indexing cortical entrainment to natural speech  
590 at the phonemic level: Methodological considerations for applied research. *Hearing*  
591 *Research*. <https://doi.org/10.1016/j.heares.2017.02.015>
- 592 Ding, N., & Simon, J. Z. (2013). Adaptive Temporal Encoding Leads to a Background-  
593 Insensitive Cortical Representation of Speech. *Journal of Neuroscience*.  
594 <https://doi.org/10.1523/jneurosci.5297-12.2013>
- 595 Ellis, C. T., & Turk-Browne, N. B. (2018). Infant fMRI: A Model System for Cognitive  
596 Neuroscience. *Trends in Cognitive Sciences*.  
597 <https://doi.org/10.1016/j.tics.2018.01.005>
- 598 Fiedler, L., Wöstmann, M., Graversen, C., Brandmeyer, A., Lunner, T., & Obleser, J.  
599 (2017). Single-channel in-ear-EEG detects the focus of auditory attention to  
600 concurrent tone streams and mixed speech. *Journal of Neural Engineering*.  
601 <https://doi.org/10.1088/1741-2552/aa66dd>
- 602 Fiedler, L., Wöstmann, M., Herbst, S. K., & Obleser, J. (2019). Late cortical tracking of

- 603 ignored speech facilitates neural selectivity in acoustically challenging conditions.  
604 *NeuroImage*. <https://doi.org/10.1016/j.neuroimage.2018.10.057>
- 605 Hamilton, L. S., & Huth, A. G. (2018). The revolution will not be controlled: natural  
606 stimuli in speech neuroscience. *Language, Cognition and Neuroscience*.  
607 <https://doi.org/10.1080/23273798.2018.1499946>
- 608 Hasson, U., Nir, Y., Levy, I., Fuhrmann, G., & Malach, R. (2004). Intersubject  
609 Synchronization of Cortical Activity during Natural Vision. *Science*.  
610 <https://doi.org/10.1126/science.1089506>
- 611 Huk, A., Bonnen, K., & He, B. J. (2018). Beyond Trial-Based Paradigms: Continuous  
612 Behavior, Ongoing Neural Activity, and Natural Stimuli. *The Journal of*  
613 *Neuroscience*. <https://doi.org/10.1523/jneurosci.1920-17.2018>
- 614 Jessen, S., & Kotz, S. A. (2011). The temporal dynamics of processing emotions from  
615 vocal, facial, and bodily expressions. *NeuroImage*, 58(2), 665–674.
- 616 Jones, E. J. H., Venema, K., Lowy, R., Earl, R. K., & Webb, S. J. (2015). Developmental  
617 changes in infant brain activity during naturalistic social experiences.  
618 *Developmental Psychobiology*. <https://doi.org/10.1002/dev.21336>
- 619 Kalashnikova, M., Peter, V., Di Liberto, G. M., Lalor, E. C., & Burnham, D. (2018).  
620 Infant-directed speech facilitates seven-month-old infants' cortical tracking of  
621 speech. *Scientific Reports*. <https://doi.org/10.1038/s41598-018-32150-6>
- 622 Lalor, E. C., Pearlmutter, B. A., Reilly, R. B., McDarby, G., & Foxe, J. J. (2006). The  
623 VESPA: A method for the rapid estimation of a visual evoked potential.  
624 *NeuroImage*. <https://doi.org/10.1016/j.neuroimage.2006.05.054>
- 625 Leong, V., Byrne, E., Clackson, K., Georgieva, S., Lam, S., & Wass, S. (2017). Speaker  
626 gaze increases information coupling between infant and adult brains. *Proceedings of*  
627 *the National Academy of Sciences*. <https://doi.org/10.1073/pnas.1702493114>
- 628 Marshall, P. J., & Shipley, T. F. (2009). Event-related potentials to point-light displays of  
629 human actions in 5-month-old infants. *Developmental Neuropsychology*.  
630 <https://doi.org/10.1080/87565640902801866>
- 631 Matusz, P. J., Dikker, S., Huth, A. G., & Perrodin, C. (2018). Are we ready for real-world  
632 neuroscience? *Journal of Cognitive Neuroscience*.  
633 [https://doi.org/10.1162/jocn\\_e\\_01276](https://doi.org/10.1162/jocn_e_01276)

- 634 Naselaris, T., Kay, K. N., Nishimoto, S., & Gallant, J. L. (2011). Encoding and decoding  
635 in fMRI. *NeuroImage*. <https://doi.org/10.1016/j.neuroimage.2010.07.073>
- 636 Nishimoto, S., Vu, A. T., Naselaris, T., Benjamini, Y., Yu, B., & Gallant, J. L. (2011).  
637 Reconstructing visual experiences from brain activity evoked by natural movies.  
638 *Current Biology*. <https://doi.org/10.1016/j.cub.2011.08.031>
- 639 O’Sullivan, A. E., Crosse, M. J., Di Liberto, G. M., & Lalor, E. C. (2017). Visual Cortical  
640 Entrainment to Motion and Categorical Speech Features during Silent Lipreading.  
641 *Frontiers in Human Neuroscience*. <https://doi.org/10.3389/fnhum.2016.00679>
- 642 Oostenveld, R., Fries, P., Maris, E., & Schoffelen, J.-M. (2011). FieldTrip: Open source  
643 software for advanced analysis of MEG, EEG, and invasive electrophysiological  
644 data. *Computational Intelligence and Neuroscience*, 2011, 156869.
- 645 Pichon, S., de Gelder, B., & Grèzes, J. (2009). Two different faces of threat. Comparing  
646 the neural systems for recognizing fear and anger in dynamic body expressions.  
647 *NeuroImage*, 47, 1873–1883.
- 648 Reid, V. M., Hoehl, S., & Striano, T. (2006). The perception of biological motion by  
649 infants: An event-related potential study. *Neuroscience Letters*.  
650 <https://doi.org/10.1016/j.neulet.2005.10.080>
- 651 Reynolds, G. D., & Guy, M. W. (2012). Brain-behavior relations in infancy: Integrative  
652 approaches to examining infant looking behavior and event-related potentials.  
653 *Developmental Neuropsychology*. <https://doi.org/10.1080/87565641.2011.629703>
- 654 Ringach, D., & Shapley, R. (2004). Reverse correlation in neurophysiology. *Cognitive  
655 Science*. <https://doi.org/10.1016/j.cogsci.2003.11.003>
- 656 Ru, P. (2001). *Multiscale Multirate Spectro-Temporal Auditory Model*. University of  
657 Maryland College Park.
- 658 Stets, M., Stahl, D., & Reid, V. M. (2012). A meta-analysis investigating factors  
659 underlying attrition rates in infant ERP studies. *Developmental Neuropsychology*,  
660 37(3), 226–252. <https://doi.org/10.1080/87565641.2012.654867>
- 661 Vanrullen, R., & MacDonald, J. S. P. (2012). Perceptual echoes at 10 Hz in the human  
662 brain. *Current Biology*. <https://doi.org/10.1016/j.cub.2012.03.050>
- 663 Webb, S. J., Long, J. D., & Nelson, C. A. (2005). A longitudinal investigation of visual  
664 event-related potentials in the first year of life. *Dev Sci*, 8(6), 605–616.

665 <https://doi.org/10.1111/j.1467-7687.2005.00452.x>

666 Wunderlich, J. L., & Cone-Wesson, B. K. (2006). Maturation of CAEP in infants and  
667 children: A review. *Hearing Research*. <https://doi.org/10.1016/j.heares.2005.11.008>

668 Wunderlich, J. L., Cone-Wesson, B. K., & Shepherd, R. (2006). Maturation of the  
669 cortical auditory evoked potential in infants and young children. *Hearing Research*.  
670 <https://doi.org/10.1016/j.heares.2005.11.010>

671